Antony V Samrot et al /J. Pharm. Sci. & Res. Vol. 10(9), 2018, 2169-2174

ISSN:0975-1459
Journal of Pharmaceutical Sciences and Research
www.jpsr.pharmainfo.in

Utilization of Crab Shell Derived Chitosan for Production of Gallic Acid Loaded Nanocomposites for Drug Delivery

Antony V Samrot[1*], Shobana N[1], Sheryl Ann Philip[1], Ujjala Burman[1], Kumar Chandrasekaran[2]

[1]Department of Biotechnology, School of Bio and Chemical Engineering, Sathyabama Institute of Science and Technology, Chennai 600119, Tamil Nadu, India
[2]Centre for Ocean Research, Sathyabama Institute of Science and Technology, Chennai 600119, Tamil Nadu, India

Abstract

Chitosan derived from crustaceans are said to be biodegradable as well as biocompatible. In this study, *Metacarcinus magister* (crab) shell derived chitosan was utilized to produce gallic acid loaded nanocomposites. The deacetylated form of chitin i.e., chitosan (CS) along with carboxymethyl cellulose (CMC) were made into nanocomposites with chelators barium chloride and sodium tripolyphosphate. Drug encapsulated (Gallic acid) nanocomposites were also prepared. The produced nanocomposites were characterized by Fourier Transform-InfraRed Spectroscopy (FTIR), Scanning Electron Microscopy (SEM) and Atomic Force Microscopy (AFM) analysis. The produced nanocomposites were also analysed for drug encapsulation efficiency, drug release kinetics and controlled drug delivery *in vitro*.

Keywords: Chitosan, gallic acid, barium chloride, sodium tripolyphosphate, Drug delivery

INTRODUCTION

Nanotechnology has a promising potential in improving targeted drug delivery which increases efficacy and reduces toxicity with proven beneficial effects to patients and also to pharma based companies by replacing the existing classical medicines in markets [1-3]. The drawbacks of conventional drug delivery system such as limited effectiveness, poor bio-distribution and lack of selectivity, this can be overcome using controlled drug delivery system (DDS), where this system provides targeted drug delivery in the body, maintains drug concentration for longer duration of time, protects the drug from rapid degradation and minimises the undesirable side effects. If these drugs are nano sized, then it can easily be taken up by the cells and targeted drug delivery is possible [4]. During the process of designing controlled release dosage formulations, choice of biopolymer is of vital importance since it acts as drug carrier [5]. Chitosan can be used as a drug carrier for many possible routes of administration as it has favourable biological properties, such as non-toxicity, biocompatibility, biodegradability, mucoadhesive and antibacterial characteristics [2, 6-9]. Chitosan is a linear polysaccharide and it is deacetylated derivative of chitin with β-[1–4]-linked D glucosamine (deacetylated unit) and N-acetyl-D-glucosamine. Chitosan contains a number of free amine groups which readily cross-links with various anions. Additionally, it can be formulated as a controlled release matrix [10, 15b]. Carboxymethyl cellulose (CMC) a naturally occurring polysaccharide is highly viscous but semi-rigid, hydrophilic, mucoadhesive, biodegradable, biocompatible and nontoxic [11-13]. At low pH, cationic chitosan reassembles with negatively charged barium chloride/sodium tripolyphosphate and carboxymethyl cellulose to form nanoparticles via ionic gelation [14, 15a]. Gallic acid (GAL) (3, 4, 5-trihydroxybenzoic acid) is a naturally occurring triphenolic compound which is found in tea leaves, grapes, oak bark, blueberries, apples and other fruits [16]. Gallic acid has been reported to show anticancer activity against leukemia [17-19], prostate cancer [20], lung cancer [21], stomach and colon cancer [22, 23], breast, cervical and esophageal cancer [24, 25]. Apart from anticancer activity, it also exhibit antibacterial, antifungal [26, 27], antioxidant [28, 29] and antidiabetic activities [30]. In this study, chelators such as barium chloride and sodium tripolyphosphate are used to synthesis chitosan – carboxymethyl cellulose based nanocomposites and it was also encapsulated with gallic acid. These polymeric nanoparticles are characterised using Fourier Transform-InfraRed Spectroscopy (FTIR), Scanning Electron Microscopy (SEM) and Atomic Force Microscopy (AFM) analysis. Drug encapsulation, drug release kinetics and *invitro* controlled drug release kinetics using agar well diffusion method are performed.

MATERIALS AND METHODS

Materials

All chemicals used in this study were of analytical grade. Nutrient media, agar powder and potassium permanganate were obtained from M/s. Hi-Media, India; barium chloride was obtained from M/s. Sisco Research Laboratories Pvt. Ltd, India; acetic acid and oxalic acid were purchased from M/s. Fisher Chemical, India; sodium tripolyphosphate (anhydrous) and drug gallic acid were purchased from M/s. Loba Chemie, India; carboxymethyl cellulose was purchased from M/s. Micro Fine Chemicals, India; ethyl alcohol AR was obtained from Changshu Yangyuan Chemicals, India. Sodium hydroxide and hydrochloric acid were obtained from M/s. Rankem, India.

Preparation of Chitosan From Crab Shells

Crab shells of *Metacarcinus magister* were obtained from Shozhinganallur fish market, Chennai, Tamil Nadu - 600119, India. The exoskeletons were scraped to remove tissues, sand and other waste and washed thrice with tap water followed by distilled water. They were then dried under direct sunlight. The dried shells were ground to powder and used for further processes. Chitosan was extracted by following the procedures of Samrot et al [15b], Yen et al [31] and Chang [32]. Depigmentation was performed for 1h using 1% potassium permanganate and 1% oxalic acid [33, 34].

Characterization of Chitosan

Fourier Transform Infrared Spectroscopy (FTIR)

The chitosan samples prepared from *Metacarcinus magister* were analysed in transmission mode scan at the spectral range between 4000 and 400cm^{-1}using IR Affinity-1s (Shimadzu, Japan) instrument.

Preparation Of Nanocomposites

Preparation of Chitosan Nanocomposites using chelators

Chitosan nanocomposites were synthesized by following the method of Samrot et al [15a, b] with a modification, the modification was as follows – while the chelators were added dropwise, chitosan (CS) was stirred vigorously using magnetic stirrer, after which 0.4% of CMC solution is also added dropwise to the mixture. 0.2% and 0.4% chelators (barium chloride and sodium tripolyphosphate) were used in this study. The samples chelated with $BaCl_2$ were labelled as 0.2B and 0.4B, whereas

samples chelated with sodium tripolyphosphate were labelled as 0.2S and 0.4S. Then the produced nanocomposites were lyophilized and stored at 4^0C.

Preparation of Gallic acid loaded Chitosan Nanocomposites
0.1% of Gallic Acid (GAL) solution was prepared in 25 ml ethanol. GAL was added to CS solution and stirred vigorously in magnetic stirrer for 10 minutes. The above illustrated methodology was followed to produce GAL loaded nanocomposites. 0.2% and 0.4% of chelators (barium chloride and sodium tripolyphosphate) were used in this study. The samples chelated with $BaCl_2$ were labelled as 0.2BG and 0.4BG, whereas samples chelated with sodium tripolyphosphate were labelled as 0.2SG and 0.4SG. Then the produced nanocomposites were lyophilized as earlier.

Characterization Of Nanocomposites
Fourier Transform Infrared Spectroscopy (FTIR)
The drug loaded and unloaded CMC-CS nanocomposites were analysed by FTIR. The pellets were prepared on a KBr press. The spectra were scanned over the wave number range of 4000 to 400 cm^{-1} using IR Affinity-1s (Shimadzu, Japan) instrument.

Scanning Electron Microscopy (SEM)
The CMC-CS nanocomposites with and without gallic acid were loaded onto carbon strips and sputter coated with gold. The sputtered samples were examined under SEM (SEI and BSI) (Carl Zeiss, Germany).

Atomic Force Microscopy (AFM)
Drug loaded and unloaded CMC-CS nanocomposites were loaded onto a cover slip and subjected for AFM (Bruker, Germany) after ultrasonication.

Drug Encapsulation Efficiency (EE)
After preparing the GAL loaded nanocomposites, it was centrifuged at 3500g at every 10min for 2h. The amount of GAL present in the supernatant was evaluated spectrophotometrically at 273nm (Absorbance maxima of Gallic acid) using UV–VIS spectrophotometer UV-1800 (Shimadzu, Japan) [35]. Triplet values were taken for each sample and the mean value was calculated. Graph was plotted taking time in minutes on the x axis and absorbance in nm on the y axis.

Drug Release Kinetics
The drug release kinetics for GAL loaded nanocomposites was studied using dialysis membrane technique [36]. Each drug loaded nanocomposites were separately dispersed in ethanol (to dissolve the CS outer shell), poured into dialysis membrane and placed separately in a solution containing 50ml of distilled water and ethanol (1:1) and left at room temperature. The amount of GAL release was measured by taking 1ml of the release medium at every 10 minutes interval for 3h. Absorbance was recorded at 273 nm. Graphs were plotted by taking time interval in minutes on the x axis and absorbance in nm on the y axis.

***Invitro* Controlled Drug Release Studies**
Anti-Bacterial Activity
The *invitro* controlled releasing ability of GAL loaded nanocomposites in presence of different solvents such as water, ethanol, PBS (pH 6.8) and acetic acid (0.1%) was evaluated using agar well diffusion method against *Pseudomonas aeruginosa* [37]. Wells were bored on solidified nutrient agar plates and four different concentrations (20µl, 40 µl, 60 µl, 80 µl) of each sample were added to the wells. After 24h of incubation, the plates were checked for zone of clearance [38].

RESULTS AND DISCUSSIONS

Characterisation of Chitosan
FTIR analysis of different functional groups of the extracted chitosan is illustrated in Figure 1. The characteristic peaks of hydroxyl group of chitosan were observed at 3593, 3570, 3315, 3197 cm^{-1}. The amide bonds of N-acetyl glucosamine were observed at the range of 1637, 1631 cm^{-1}. The C=O stretching was observed at the range of 1670 cm^{-1}. The characteristic peaks at the range of 1568, 1581 and 1587 cm^{-1} revealed the N-H bending vibrations. CH_2 wagging was observed at the range of 1338 cm^{-1}. The characteristic peaks coincided with the results obtained by Sarbon et al [39].

Characterization of Nanocomposites
Fourier Transform Infrared Spectroscopy (FTIR) analysis of nanocomposites
FTIR analysis of prepared nanoparticle (Figure 2 & 3) revealed the functional groups corresponding to CS, CMC, GAL, TPP and $BaCl_2$. The characteristic peaks of hydroxyl group of chitosan were observed in the range of 3373, 3379, 3396 cm^{-1} in all the produced nanocomposites. The amide bond present in the structure of N-acetyl glucosamine was viewed as bending vibrations of NH_2 in the range of 1637, 1631, 1613 cm^{-1} in all the nanocomposites. The NH_2 of CMC was shifted to 1613, 1627, 1600, and 1626 cm^{-1} in 0.2SG, 0.2BG, 0.2BG and 0.4BG from 1567, 1566, 1581 and 1564 cm^{-1} and for 0.2S, 0.2B, 0.4S and 0.4B indicating the overlapping of C=N confirming the formation of chitosan-carboxymethyl cellulose schiffs base material. All the GAL loaded nanocomposites were found to show C=O band of GAL near 1690 to 1630 cm^{-1}nanocomposites (Figure 2b, d and Figure 3 b, d) [40]. Peaks around 3600$cm^{-1}$was for the OH stretching of benzene ring of GAL loaded nanocomposites (Figure 2b, d and Figure 3 b, d). The characteristic peaks for the chelators were also as reported earlier [15].

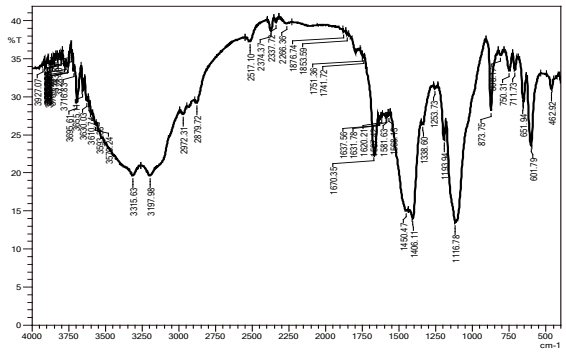

Figure1: FTIR Spectroscopy analysis of the extracted chitosan

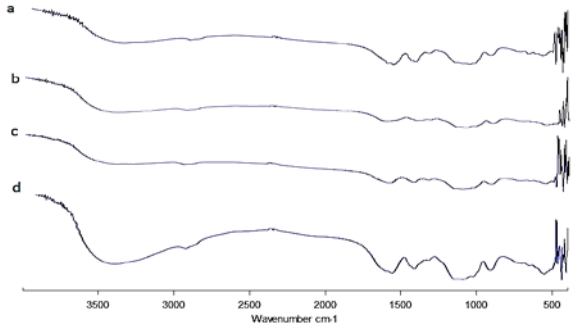

Figure 2: FTIR spectroscopy analysis of chitosan nanocomposites chelated with TPP and loaded with Gallic acid. a) 0.2S, b) 0.2SG, c) 0.4S, d) 0.4SG

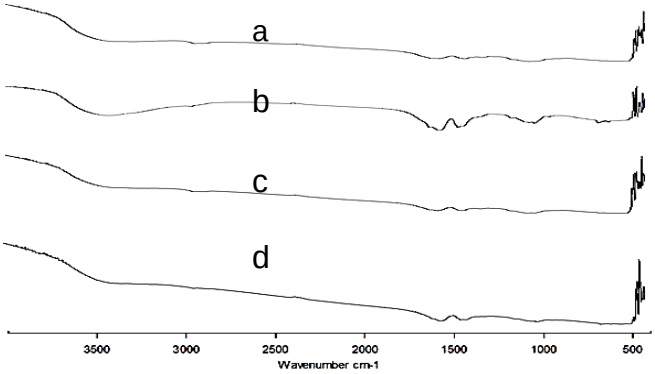

Figure 3: FTIR spectroscopy analysis of chitosan nanocomposites chelated with $BaCl_2$ and loaded with Gallic acid. a) 0.2B, b) 0.2BG, c) 0.4B, d) 0.4BG

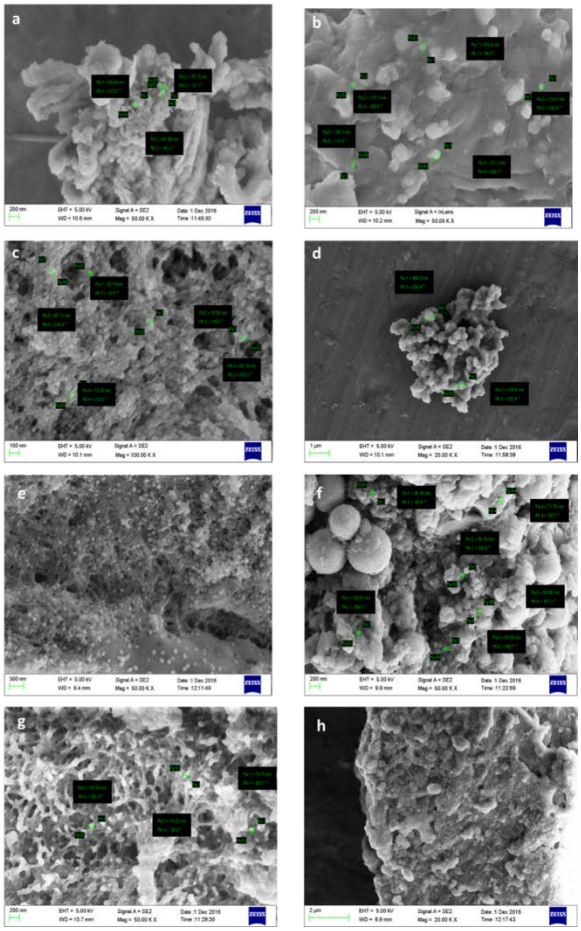

Figure 4: Scanning Electron Microscopy analysis of CS-CMC nanocomposites chelated with TPP and $BaCl_2$. a)0.2S, b) 0.2SG, c)0.4S, d)0.4SG, e)0.2B, f) 0.2BG, g) 0.4B, h) 0.4BG

Scanning Electron Microscopy (SEM)

0.2% chelated with sodium tripolyphosphate appeared to be spherical to irregular and the composites were fluffy in appearance of size range 78 – 88 nm (Figure 4a). The gallic acid loaded composites i.e. 0.2SG appeared spherical shape with non-uniform distribution in size ranging from 100 to 171 nm (Figure 4b). Drug encapsulation might have increased the size of the composites. Whereas 0.4% TPP chelated composites showed a uniform distribution with size range 25 – 70 nm (figure 4c), whereas 0.4SG had high aggregations with size ranging above 300 nm (figure 4d). Increasing the concentration of chelators and pH have been reported to influence the size of particles [15a, 41]

The gallic acid loaded samples such as 0.2BG (figure 4g) and 0.4BG (figure 4h) were regular and spherical in shape. Among them, the lower concentration of $BaCl_2$ which is 0.2BG showed spherical particles with mildly even distribution of particle of size 55 – 71nm whereas the later i.e. 0.4BG showed aggregated and unevenly sized particles of 74 – 82 nm range. $BaCl_2$ is reported to produce smaller particles than sodium tripolyphosphate [15a].

Atomic Force Microscopy (AFM)

AFM analysis confirmed that the size of GAL loaded nanocomposites and it is on par with the SEM analysis (Figure 5).

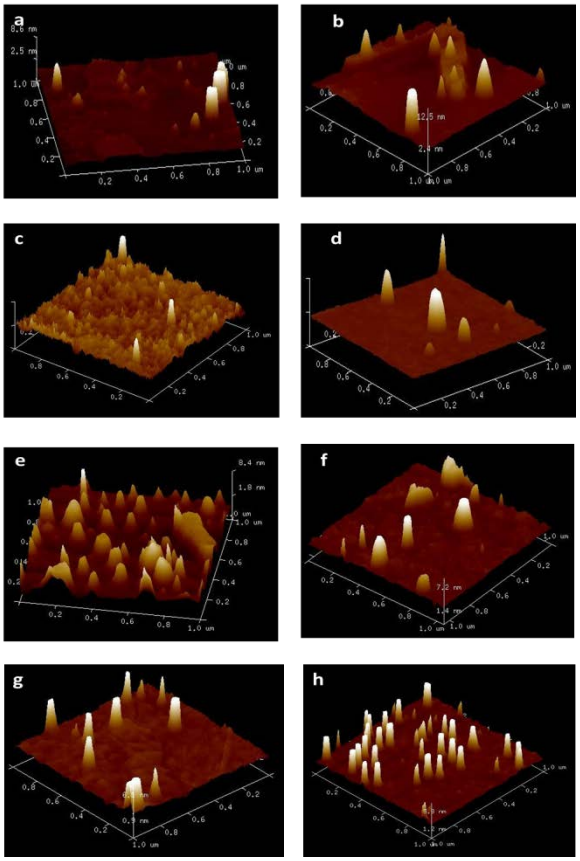

Figure 5: Atomic Force Microscopy analysis of CS-CMC nanocomposites chelated with TPP and $BaCl_2$. a) 0.2S, b) 0.2SG, c) 0.4S, d) 0.4SG, e) 0.2B, f) 0.2BG, g) 0.4B, h) 0.4BG

Drug Encapsulation Efficiency (EE)

The encapsulation efficiency of GAL on CS-GAL nanocomposites was found to be time dependent. The nanocomposites loaded with GAL and chelated with 0.2% and 0.4% TPP showed proper encapsulation. But in contrast, nanocomposites chelated with 0.4% $BaCl_2$ (figure 6) showed high variations with zig-zag progression. Encapsulation efficiency of lower concentration i.e. 0.2% $BaCl_2$ was found to remain steady until the 90^{th} minute only which then followed an improper progression.

Drug Release Kinetics

0.4SG was stable in releasing the drug till the 70^{th} minute (figure 7). A sudden burst of drug release was observed at 80^{th} to 90^{th} minute which then dropped and was releasing the drug till 180^{th} minute. Earlier report of curcumin release by TPP chelated microparticles was found to be irregular [15]. When barium chloride was used as chelator, it was releasing the drug slowly till 180^{th} minute (Figure 7). 0.6% $BaCl_2$ chelated CS microparticles were reported to release curcumin very steadily till 3h [15a].

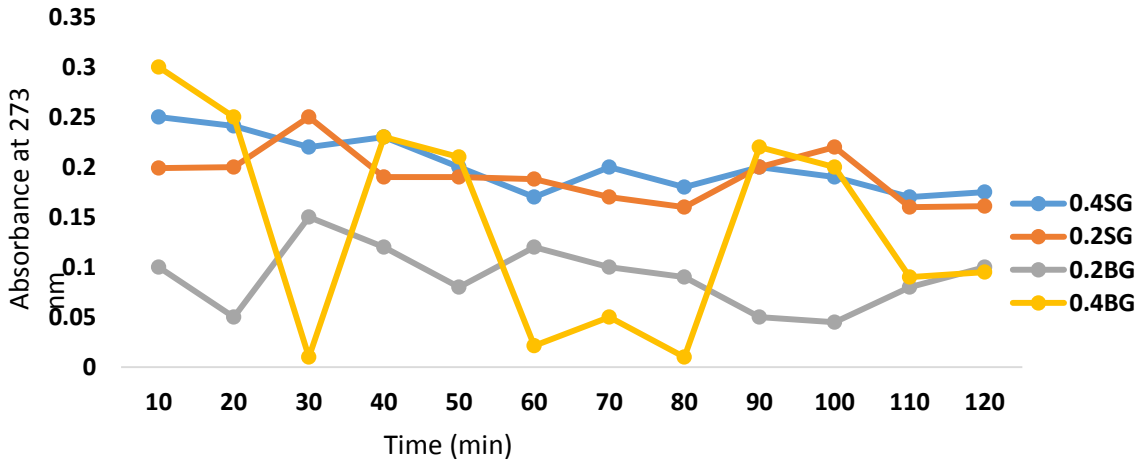

Figure 6: Gallic acid Encapsulation Efficiency of CS-CMC nanocomposites chelated with different concentrations of TPP and $BaCl_2$

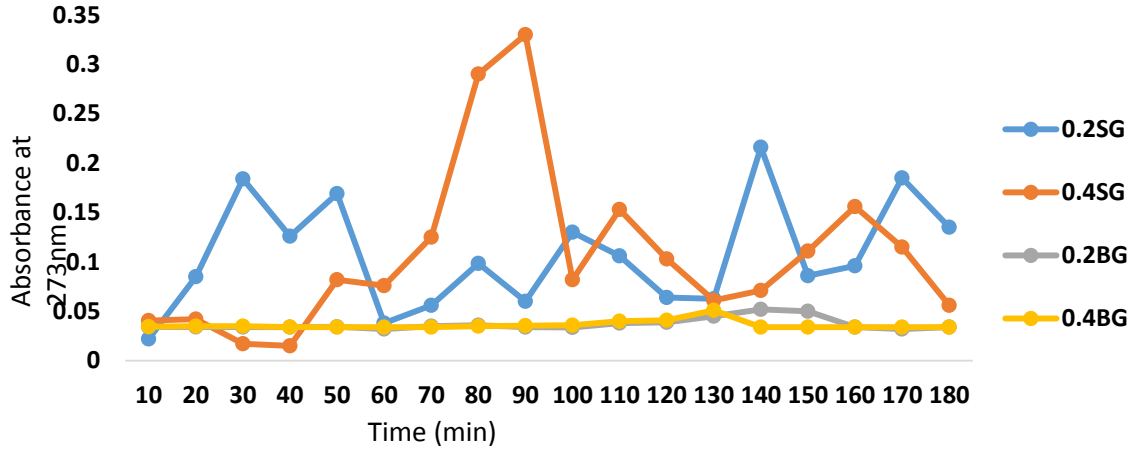

Figure 7: Gallic acid Release kinetics of CS-CMC nanocomposites chelated with different concentrations of TPP and $BaCl_2$

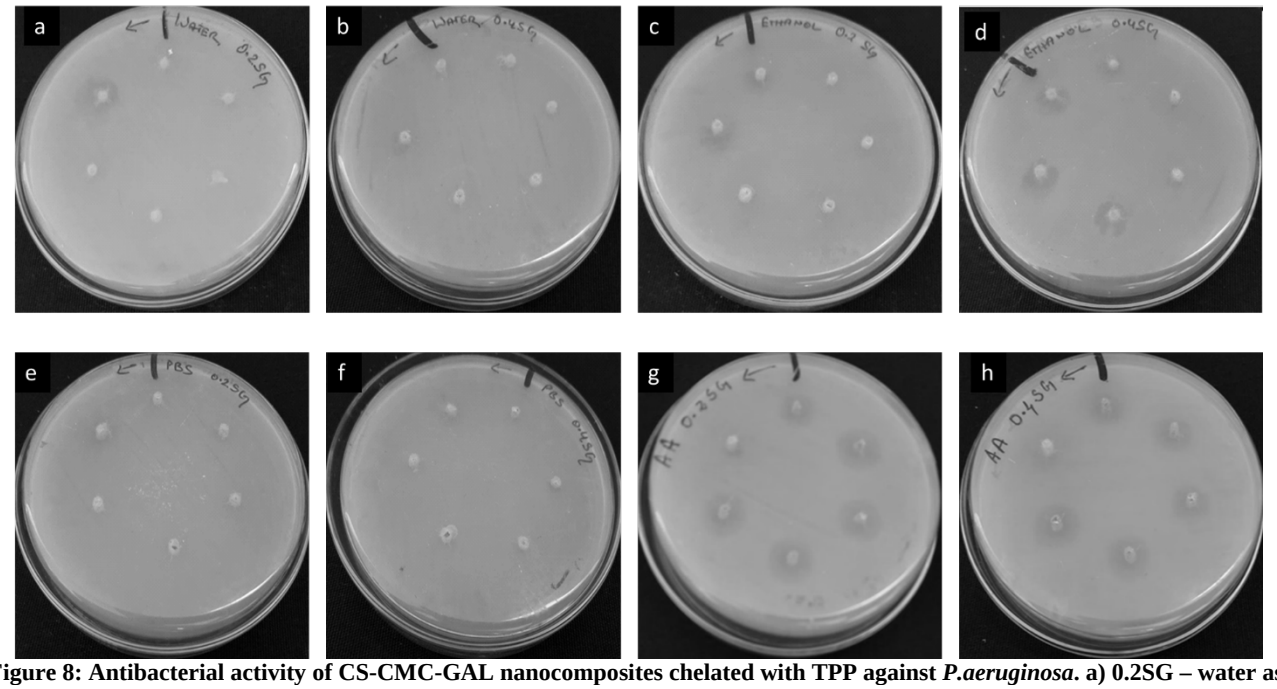

Figure 8: Antibacterial activity of CS-CMC-GAL nanocomposites chelated with TPP against *P.aeruginosa*. a) 0.2SG – water as solvent, b) 0.4SG – water as solvent, c) 0.2SG – ethanol as solvent, d) 0.4SG – ethanol as solvent, e) 0.2SG – PBS as solvent, f) 0.4SG – PBS as solvent, g) 0.2SG – 0.1% acetic acid as solvent, h) 0.2SG – 0.1% acetic acid as solvent

Table 1: Antibacterial activity of chitosan nanocomposites chelated with TPP and loaded with gallic acid against *P.aeruginosa*

Type of nanocomposites	Solvents	Zone of inhibition at various Concentration (in cm)			
		20µl	40 µl	60 µl	80 µl
0.2% TPP	Water	-ve	-ve	-ve	-ve
0.4% TPP		-ve	-ve	-ve	-ve
0.2% TPP	PBS	-ve	-ve	-ve	-ve
0.4% TPP		-ve	-ve	-ve	-ve
0.2% TPP	Ethanol	-ve	-ve	-ve	1.3
0.4% TPP		-ve	0.6	0.8	0.9
0.2% TPP	Acetic acid	0.5	0.6	0.8	0.9
0.4% TPP		0.5	0.6	0.8	0.9

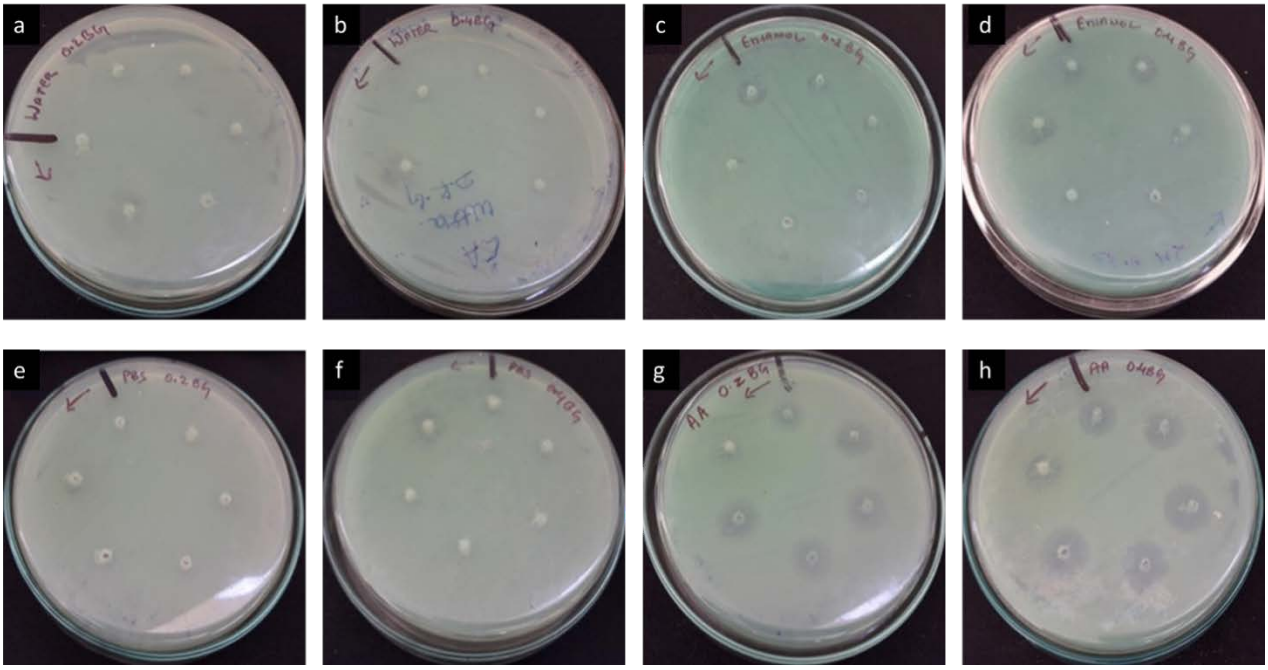

Figure 9: Antibacterial activity of CS-CMC-GAL nanocomposites chelated with $BaCl_2$ against *P.aeruginosa*. a) 0.2BG – water as solvent, b) 0.4BG – water as solvent, c) 0.2BG – ethanol as solvent, d) 0.4BG – ethanol as solvent, e) 0.2BG – PBS as solvent, f) 0.4BG – PBS as solvent, g) 0.2BG – 0.1% acetic acid as solvent, h) 0.2BG – 0.1% acetic acid as solvent

Table 2: Antibacterial activity of chitosan nanocomposites chelated with $BaCl_2$ and loaded with gallic acid against *P.aeruginosa*

Type of nanocomposites	Solvents	Zone of inhibition at various Concentration (in cm)			
		20µl	40 µl	60 µl	80 µl
0.2% BG	Water	-ve	-ve	-ve	-ve
0.4% BG		-ve	-ve	-ve	-ve
0.2% BG	PBS	-ve	-ve	-ve	-ve
0.4% BG		-ve	-ve	-ve	-ve
0.2% BG	Ethanol	0.2	0.2	0.3	0.5
0.4% BG		-ve	-ve	-ve	0.5
0.2% BG	Acetic acid	0.2	0.5	0.8	1.1
0.4% BG		0.5	0.5	0.8	1.1

***In Vitro* Controlled Release Studies**

Anti-Bacterial Activity

The antibacterial activity was performed for the prepared nanocomposites using four different solvents water, ethanol, PBS (pH 6.8) and acetic acid (0.1%). The activity was observed when ethanol and acetic acid, but the highest zone was observed using acetic acid as solvent for GAL loaded samples. When ethanol was used, 0.5cm of zone inhibition was observed in nanocomposites chelated with $BaCl_2$ i.e. 0.2BG, 0.4BG (Figure 9 and Table 2) and 1.3cm for 0.2SG (Figure 8 and Table 1). But when acetic acid was used, highest zone of inhibition was found in nanocomposites 0.2BG, 0.4BG of 1.1cm and 0.9cm by 0.2SG and 0.4SG (Figure 8, 9 and Table 1, 2). From this, it is evident that nonpolar solvent could release the encapsulated drug. Similar results were obtained by Samrot et al [15b].

SUMMARY AND CONCLUSION

Chitosan was extracted from *Metacarcinus magister* crab shells and was characterised using FTIR which was found to be pure chitosan with all functional groups. It was utilized for the synthesis of chitosan nanocomposites using carboxymethyl cellulose chelated with barium chloride and sodium tripolyphosphate with two different concentrations (0.2% and 0.4%). The FTIR of the nanocomposites showed characteristic

bonds associated to CMC, CS, GAL, TPP and $BaCl_2$. The SEM analysis indicated the size of the nanocomposites to be less than 200nm. The encapsulation efficiency was found to be time dependent. The 0.4% TPP chelated nanoparticle had higher encapsulation efficiency than barium chloride. The encapsulated drug was found to be released *invitro* only when ethanol and acetic acid was used as solvent.

REFERENCE:

1. Mitra A, Dey B. Chitosan microspheres in novel drug delivery systems. Indian J Pharm Sci. 2011, 73(4): 355–366.
2. Agnihotri SA, Mallikarjuna NN, Aminabhavi TM. Recent advances on chitosan-based micro- and nanoparticles in drug delivery. J Control Release. 2004, 100, 5–28.
3. Soppimath KS, Aminabhavi TM, Kulkarni AR, Rudzinski WE. Biodegradable polymeric nanoparticles as drug delivery devices. J Control Release. 2001, 70, 1–20.
4. Wilczewska AZ, Katarzyna N, Karolina HM, Halina C. Nanoparticles as drug delivery systems. Pharma Reports. 2012, 64, 1024.
5. Kas HS. Chitosan: Properties, preparations and application to microparticulate systems. J Microencapsul. 1997, 14, 689–711.
6. Goy RC, de Britto D, Assis OBG. A review of the antimicrobial activity of chitosan. Polim Ciência E Tecnol. 2009, 19, 241–7
7. Wazed SA, Joshi M, Rajendran S. Modulation of size, shape and surface charge of chitosan nanoparticles with reference to antimicrobial activity. Adv Sci Lett. 2010, 3, 452–60
8. Begoña CG, Duncan R. Evaluation of the biological properties of soluble chitosan and chitosan microspheres. Int J Pharm. 1997, 148, 231–240.
9. Dudhani AR, Kosaraju SL. Bioadhesive chitosan nanoparticles: Preparation and characterization. Carbohydrate Polymers. 2010, 81(2):243-251. Udoi:10.1016/j.carbpol.2010.02.026
10. Stolnik S, Shakesheff K. Formulations for delivery of therapeutic proteins. BiotechnolLett. 2009, 31, 1–11.
11. Smart JD, Kellaway ID, Worthington HEC. An *in vitro* investigation of mucosa-adhesive materials for use in controlled drug delivery. J Pharm Pharmacol. 1994, 36(5):295–299
12. Zhang L, Jin Y, Liu H, Du Y. Structure and control release of chitosan/carboxymethyl cellulose microcapsules. Journal of Applied Polymer Science. 2001, 82(3):584–592
13. Sainitya R, Sriram M, Kalyanaraman V, Dhivya S, Saravanan S, Vairamani M, Sastry TP, Selvamurugan N. Scaffolds containing chitosan/carboxymethyl cellulose/mesoporous wollastonite for bone tissue engineering. International Journal of Biological Macromolecules. 2015, 80, 481–488
14. Bugnicourt L, Ladavière C. Interests of chitosan nanoparticles ionically cross-linked with tripolyphosphate for biomedical applications. Progress in Polymer Science. 2016. 60, 1–17
15. a) Samrot AV, Akanksha, Jahnavi T, Padmanaban S, Philip SA, Burman U, Rabel AM. Appl Nanosci. 2016, 6, 1219. doi:10.1007/s13204-016-0536
    b) Samrot AV, Burman U, Philip SA, Shobana N, Chandrasekaran K. Informatics in Medicine Unlocked. 2018, 10, 159-182
16. Verma S, Singh A, Mishra, A. Gallic acid: Molecular rival of cancer. Environmental Toxicology and Pharmacology. 2013, 35, 473–485
17. Inoue M, Sakaguchi N, Isuzugawa K, Tani H, Ogihara Y. Role of reactive oxygen species in gallic acid-induced apoptosis. Biol. Pharm. Bull. 2000, 23, 1153–1157.
18. Sakaguchi Y, Inoue M, Ogihara Y. Reactive oxygen species and intracellular Ca2+, common signals for apopotosis induced by gallic acid. Biochem. Pharmacol. 1998, 55, 1973–1981.
19. Saeki K, You A, Isemura M, Abe I, Seki T, Noguchi H. Apoptosis inducing activity of lipid derivatives of gallic acid. Biol. Pharm. Bull. 2000, 23, 1391–1394.
20. Veluri R, Singh RP, Liu Z, Thompson JA, Agarwal R, Agarwal C. Fractionation of grape seed extract and identification of gallic acid as one of the major active constituents causing growth inhibition and apoptotic death of DU145 human prostate carcinoma cells. Carcinogenesis. 2006, 27, 1445–1453.
21. Ji BC, Hsu WH, Yang JS, Hsia TC, Lu CC, Chiang JH, Yang LJ, Lin CH, Lin JJ, Suen LJW, Wood WG, Chung JG. Gallic acid induces apoptosis via caspase-3 and mitochondrion-dependent pathways in vitro and suppresses lung xenograft tumor growth in vivo. J. Agric. Food Chem. 2009, 57, 7596–7604.
22. Giftson JS, Jayanthi S, Nalini N. Chemopreventive efficacy of gallic acid, an antioxidant and anticarcinogenic polyphenol, against 1, 2-dimethyl hydrazine induced rat colon carcinogenesis. Invest. New Drugs. 2010, 28, 251–259.
23. Sohi KK, Mittal N, Hundal MK, Khanduja KL. Gallic acid, an antioxidant, exhibits antiapoptotic potential in normal human lymphocytes: A Bcl-2 independent mechanism. J. Nutr. Sci. Vitaminol. 2003, 49, 221–227.
24. Faried A, Kurnia D, Faried LS, Usman N, Miyazaki T, Kato H, Kuwano H. Anticancer effects of gallic acid isolated from Indonesian herbal medicine, *Phaleria macrocarpa* (Scheff.) Boerl, on human cancer cell lines. Int. J. Oncol. 2007, 30, 605–613.
25. You BR, Moon HJ, Han YH, Park WH. Gallic acid inhibits the growth of HeLa cervical cancer cells via apoptosis and/or necrosis. Food Chem. Toxicol. 2010, 48, 1334–1340.
26. Arunkumar S, Ramalakshmi N, Saraswathi T, Aruloly L. Synthesis, Characterisation and Biological Evaluation of some novel 2, 5-disubstituted- 1, 3, 4-oxadiazole derivatives of Gallic acid. 2006, Indian J Heterocycl. Chem. 16, 29–32.
27. Strippoli V, D'Auria FD, Tecca M, Callari A, Simonetti G. Propyl gallate increases in vitro antifungal imidazole activity against *Candida albicans*. Int. J. Antimicrob. Agents. 2000, 16, 73–76.
28. Khan NS, Ahmad A, Hadi SM. Anti-oxidant, pro-oxidant properties of tannic acid and its binding to DNA. Chem. Biol. Interact. 2000, 125, 177–189
29. Zheng W, Wang SY. Antioxidant activity and phenolic compounds in selected herbs. J. Agric. Food Chem. 2001, 49, 5165–5170
30. Purbowatiningrum, Ngadiwiyana, Ismiyarto, Fachriyah E, Eviana I, Eldiana O, Amaliyah N, Sektianingrum. Antidiabetic Activity from Gallic Acid Encapsulated Nanochitosan IOP Conf. Series: Materials Science and Engineering. 2017, 172, 012042
31. Yen MT, Yang JH, Mau JL. Physicochemical characterization of chitin and chitosan from crab shells. Carbohydrate Polymers. 2009, 75, 15–21
32. Chang CT. Studies on the use of crab chitin as a water-insoluble support for the immobilization of pineapple stem bromelain and the preparation of some affinity adsorbents for proteinase. Journal of the Chinese Agricultural and Chemical Society. 1982, 20, 45–60
33. Rashmi SH, Mahendra, Biradar B, Maladkar K, Kittur AA. Extraction of chitin from prawn shell and preparation of chitosan. Res J. Chem. Environ. Sci. 2016, 4 (4S):70-73
34. Kumari S, Rath PK. Extraction and Characterization of Chitin and Chitosan from (*Labeo rohit*) Fish Scales. Procedia Materials Science. 2014, 6, 482 – 489
35. Pawar NP, Salunkhe VR. Development and validation of UV spectrophotometric method for simultaneous estimation of rutin and gallic acid in hydroalcoholic extract of *Triphalachurna*. International Journal of PharmTech Research. 2013, 5(2):724-729
36. Rajan M, Raj V. Encapsulation, characterization and In-vitro release of anti-tuberculosis drug using chitosan – poly ethylene glycol nanoparticles. Int J Pharm Sci. 2012, 4(4):255-259
37. Andres Y, Giraud L, Gerente C, Cloirec PL. Antibacterial Effects of Chitosan Powder: Mechanisms of Action. Journal Environmental Technology. 2010, 28(12).
38. Cruickshank R, 1962. Hand book of Bacteriology. 394.
39. Sarbon NM, Sandanamsamy, Kamaruzaman SFS, Ahmad F. Chitosan extracted from mud crab (*Scylla olivicea*) shells: physicochemical and antioxidant properties. J Food Sci Technol. 2015, 52(7):4266-4275
40. Hirun N, Dokmaisrijan S, Tantishaiyakul V. Experimental FTIR and theoretical studies of gallic acid–acetonitrile clusters. Spectrochimica Acta Part A. 86, 2012, 93–100.
41. Martins AF, de Oliveira DM, Pereira AGB, Rubira AF, Muniz EC. Chitosan/TPP microparticles obtained by microemulsion method applied in controlled release of heparin. Int J Biol Macromol. 2012, 51(5):1127–1133.